ChemComm

Accepted Manuscript

This article can be cited before page numbers have been issued, to do this please use: S. Xiong, J. Tao, Y. Wang, J. Tang, C. Liu, Q. Liu, Y. Wang, G. Yu and C. Pan, *Chem. Commun.*, 2018, DOI: 10.1039/C8CC04242J.

ROYAL SOCIETY OF CHEMISTRY

rsc.li/chemcomm

View Article Online
DOI: 10.1039/C8CC04242J

Journal Name

COMMUNICATION

Uniform poly(phosphazene-triazine) porous microspheres for highly efficient iodine removal

Received 00th January 20xx,
Accepted 00th January 20xx

DOI: 10.1039/x0xx00000x

www.rsc.org/

Shaohui Xiong,[a] Jian Tao,[a] Yuanyuan Wang,[a] Juntao Tang,[a] Cheng Liu,[b] Qingquan Liu,[c] Yan Wang,[a] Guipeng Yu,*[a, b] and Chunyue Pan*[a]

Rich heteroatom-doped conjugated nanoporous polymers with uniform microspherical morphology exhibit remarkablly high capacity up to 450 wt% in removing iodine from vapor phase (at 348 K and atmosphere pressure).

Volatile radio nuclides including iodine (^{129}I or ^{131}I), as a vital environmental issue, were released primarily from the waste streams of nuclear operations and medical diagnosis.[1-2] Owing to its radiotoxicity, high mobility and long-lived time, capture and sequester of such volatile component have already been regarded as key issues that desperately to be addressed.[3-4] To date, several strategies have been proposed to remove the iodine contaminants, including dry dedusting, chemical precipitation, and physical adsorption.[5] Among them, physical adsorption, which is adopted as the primary choice, features an attractive balance of general applicability, inexpensive cost, simple and rapid operation procedure. Various solid sorbents like activated carbon [6], inorganic porous materials [7], metal-organic frameworks (MOFs) [8-9] and porous organic polymers (POPs) [10-15], have been intensively explored for capturing volatile iodine molecules. Among them, POPs appear to be most promising over their inorganic counterparts because of their excellent physical/chemical stability along with tunable skeletons. [16-17] However, the practical applications of POPs constructed solely from light elements like carbon and hydrogen as iodine adsorbents still face great challenges concerning their low iodine capacity, which are attributed to the weak affinity towards guest iodine molecular. The exploring and assembly of task-specific POPs for efficient iodine capturing remains a contemporary field of materials chemistry.

Improving the loading amount of iodine in POPs can be achieved through incorporating high-affinity binding sites or task-specific designing on pore structure. Generally, the heteroatoms (nitrogen, sulfur, phosphorus, boron) densely integrated in the networks were regarded as effective sorption sites [18-22]. Through incorporating B-containing ionic bond into the skeleton, Zhu *et al.* developed charged porous aromatic frameworks which exhibit high affinity for iodine, with the loading amount up to 276 wt%.[23] Well-selected porous architectures and morphologies of sorbents act as positive factors for iodine adsorption as well.[24-25] Macroscopically honeycomb-like morphology and hierarchical porosities might be advantageous to improve the iodine uptake capacity.[26] Additionally, it was found out that the extended π–conjugations can prominently enhance the affinity of the porous solid adsorbents towards gust molecules such as H_2 and CO_2 through increasing aromatic π-surface area with ample aromatic rings, therefore leading to a remarkably high capacity.[27] However, the effect of extended π–conjugations on host-I_2 affinity remains unclear.

Inspired by the forehead mentioned work, we set out to design and prepare two types of heteroatom-rich POPs with extended π–conjugations, aiming at highly efficient removal of I_2. A mild catalyst-free method and one-pot polymerization processes were employed to fabricate POPs with extended π-conjugated backbone (denoted as **MelPOP-2** and **TatPOP-2**) from cost-effective raw materials (hexachlorocyclotriphosphazene, melamine and 4,4',4''-(1,3,5-triazine-2,4,6-triyl) trianiline). The advantages of the as-made networks are obvious. Firstly, the rich heteroatoms (such as phosphorus and nitrogen) containing frameworks may provide enhanced interactions between I_2 and POPs, and subsequently increase the I_2 loading amount. Furthermore, employing a variety of large p-π conjugated units provides a number of possibilities to interact with iodine, thus providing another possible pathway to promote the iodine affinity. As expected, the POPs networks exhibit satisfying stability, and more importantly, delivers ultrahigh iodine uptake. Upon exposure to iodine vapor at 348 K and 1.0 bar, **TatPOP-2** possesses an iodine uptake of 450 wt%. To the best of our knowledge, this number is the highest for amorphous materials that have been

[a] College of Chemistry and Chemical Engineering, Hunan Provincial Key Laboratory of Efficient and Clean Utilization of Manganese Resources, Central South University, Changsha 410083, China. E-mail: gilbertyu@csu.edu.cn, panchunyue@csu.edu.cn
[b] State Key Laboratory of Fine Chemicals, Dalian University of Technology, Dalian 116012, China.
[c] Institute of Materials Science and Engineering, Hunan University of Science and Technology, Xiangtan 411201, China.
Electronic Supplementary Information (ESI) available: [details of any supplementary information available should be included here]. See DOI: 10.1039/x0xx00000x

View Article Online
DOI: 10.1039/C8CC04242J

reported to date. [28] Surprisingly, the uptake of iodine for **TatPOP-2** reached an average of 12 wt% per unit BET specific surface area (SBET), which surpasses all known solid sorbents ever reported for I_2 adsorption. [29-33]

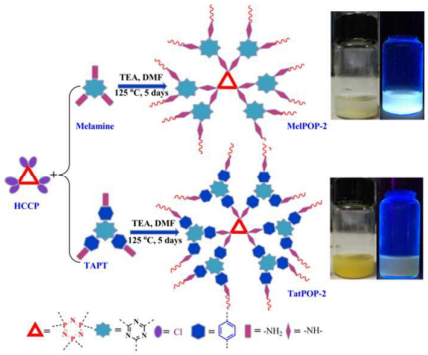

Scheme 1 Schematic of the synthesis of POPs networks for iodine removal

MelPOP-2 was synthesized from a mixture of hexachlorocyclotriphosphazene (HCCP) and melamine (1:2 molar ratio) in anhydrous *N,N*-dimethylformamide in a sealed glass ampoule by using triethylamine as base. The mixture was heated at 125 °C for 5 days and pale white powder can be obtained. The khaki powder, **TatPOP-2**, was synthesized from HCCP and 4,4',4''-(1,3,5-triazine-2,4,6-triyl) trianiline (TAPT) according to the same procedure. The thermogravimetric (TGA) analysis reveals that the synthesized samples are quite stable and no obvious weight loss when heated to 365 °C under N_2 atmosphere (Fig S1 ESI†). When comparing to HCCP, the Fourier transforms infrared (FT-IR) spectra (Fig. 1a) of our networks exhibit dramatic decrease at 522 and 601 cm^{-1}, indicating the almost complete conversion of P-Cl.

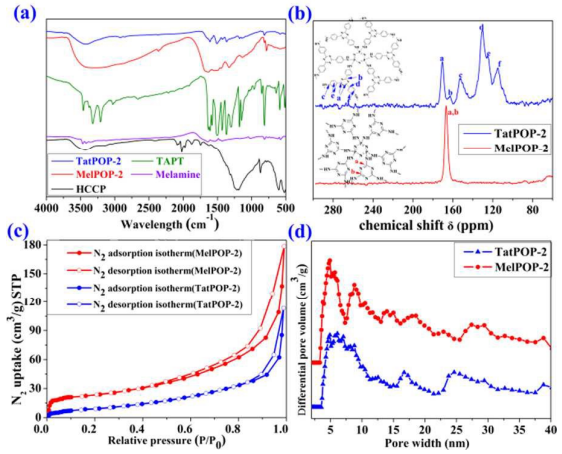

Fig. 1 a) FTIR spectra; b) Solid ^{13}C CP/MAS NMR spectra; c) N_2 adsorption-desorption isotherms curves at 77K; d) Pore size distribution curves were calculated using non-local density functional theory (NLDFT) for POPs.

The structures of POPs were further confirmed by solid-state ^{13}C NMR spectroscopy (Fig. 1b). According to X-ray photoelectron spectroscopy (XPS) analysis, P is de-convoluted into two sub-peaks located at 133.3 and 134.4 eV, which can be assigned to P-N and N-P=N, respectively (Fig S2, ESI†).[34] Additionally, energy dispersive X-ray spectroscopy (EDS) measurements manifest negligible Cl (0.08-0.11 wt %) in the networks (Fig. S3, ESI†), which demonstrates the successful reactions and high degree of polymerizations. Shown in Fig 2(a) (b) is the morphology of the networks captured by scanning electron microscopy (SEM), of which both **MelPOP-2** and **TatPOP-2** display agglomerated spherical shape with an average size ranging from 2 to 8 μm. Further characterization by high-resolution transmission electron microscopy (HR-TEM Fig. 2c, d, Fig S4) showed that the microspheres consist of abundant pores. The broad diffraction peaks can be observed in powder X-ray diffractions, indicating the amorphous nature of the POPs (Fig. S5, ESI†). The solid fluorescence spectra of **MelPOP-2** and **TatPOP-2** exhibit a maximum emission at around 436 nm and 330 nm, respectively (Fig. S6 ESI† and scheme 1). These strong fluorescence properties might be caused by the extended conjugated networks with strong electron-accepting units and altitudinal symmetry of the triazine and phosphazene units. [35-36]

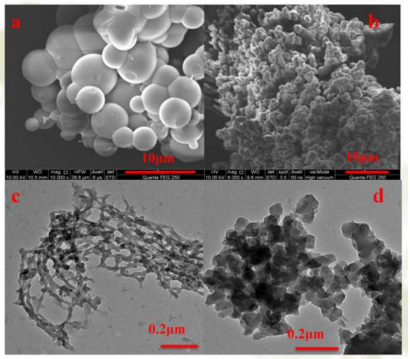

Fig. 2 The SEM images of a) **MelPOP-2**, b) **TatPOP-2**; The TEM images of c) **MelPOP-2**, d) **TatPOP-2**.

The pore features of POPs was probed by N_2 adsorption-desorption experiments at 77 K up to 1 bar. The adsorption curves can be defined as type IV isotherm on the basis of the IUPAC manual [37] (Fig. 1c), indicating the existence of mesopores **(**ESI†,Table S1**)**. Brunauer-Emmett-Teller (BET) surface areas calculated from the adsorption branch of the N_2 isotherms are 50.5 for **MelPOP-2** and 36.5 m^2/g for **TatPOP-2**, respectively. Multiple attempts to generate larger-surface-area porous polymers under different polymerization conditions (solvents, acid agent, the reaction temperature and time) failed, and the samples were gained with low BET surface areas. Hereafter, synthesis and optimal screening of polymers with a maximum reaction extent were utilized, which have been successfully confirmed by FT-IR (Fig. 1a) and EDS (Fig. S3, ESI†). The total pore volumes are 0.22 cm^3/g for **MelPOP-2** and 0.18 cm^3/g for **TatPOP-2**, respectively. The pore size distributions obtained using the nonlocal density functional theory (NLDFT) demonstrates that the pores are mainly centered at around 5 nm and 10 nm (Fig. 1d).

Based on the definite construction of the porous networks, iodine capturing capacity was studied. Iodine vapour uptake capacities of POPs were investigated by gravimetric method in a sealed vessel at 75 °C and atmosphere pressure (more detail refers to ESI†). The iodine loading capacities were measured using electronic balance at

View Article Online
DOI: 10.1039/C8CC04242J

various time intervals (Fig. 3a). The amount of loaded iodine increases gradually at initial 8 h and the adsorption reaches its saturated state after 12 h (Fig. 3a). The samples darkened gradually, which indicates that I_2 has diffused to the surface or frameworks (Fig. 3a, inset). Despite of their low BET surface areas, the iodine uptake capacities are calculated to be 450 wt% and 262 wt% for **TatPOP-2** and **MelPOP-2**, respectively. Such capacities are superior to that of subtotal porous solid absorbents including inorganic absorbents, MOFs and amorphous POPs (The detailed comparisons were summarized in Table S2, ESI†). As presented in Fig.3c, the samples exhibit pronounced iodine adsorption per unit SBET. The different per unit adsorption ability towards I_2 provides a basis for the selective capture of iodine from volatile waste streams. In these polymers, **TatPOP-2** possessed the highest adsorption capacity and efficiency toward iodine (Fig. 3c) and the data is larger than most know POPs like **SIOC-COF-7**[25] and **HCMP-3**[38]. The ultrahigh iodine uptake, especially per unit area iodine uptake of samples (12 wt%, Fig 3c or Table S2, ESI†) may be attributed to two factors. 1) The incorporation of abundant heteroatoms (N content up to 44 % for **MelPOP-2** and 15 % for **TatPOP-2**, Table S3) into frameworks can enhance the interactions between iodine molecular and frameworks. 2) Both the amine-linkages and extended π-conjugated systems with plenty of amino, highly unsaturated π-bond-rich (e.g. triazine rings and phosphazene rings) could contribute to highly efficient iodine uptakes. Pore parameters such as surface area, void pore volume and pore size distribution all influence the iodine vapor adsorption. [20] Large surface areas and ultrahigh pore volume are considered to facilitate the improvement of iodine adsorption. Meanwhile, the mesopores portion can supply effective transport pathways, and the micropores portion provides the dominant adsorption sites for iodine. [19] In many cases, however, the iodine adsorption for a POPs is not proportional to their specific surface areas and microspore volume. [28] Interestingly, **TatPOP-2**, with lower BET surface area and content of heteroatoms has been found to exhibit higher iodine adsorption than **MelPOP-2**. This trend is contrary to the earlier reports [39-40] in which the high-BET-surface-area and heteroatom-rich solids always deliver better performance on removing iodine vapours. The iodine capture capacity can be principally ascribed to the synergic effect of surface area and the following two factors i.e. the presence of abundant heteoatoms and extended conjugated system. More importantly, our results indicate that the conjugated π electrons-rich aromatic system might play a vital role in improving the iodine adsorption amount.[22],[38] The potential intermolecular-interactions between I_2 and π-electron structures provide a single route for iodine molecules to access and be restricted within well-regulated narrow limits within the nanochannels, inducing n→σ* charge transfer (CT).[41-42] The existence form of iodine captured by POPs was further ascertained by XPS (Fig. S8, ESI†). The split peaks are attributed to the iodine 3d 3/2 and 3d 5/2 orbital level. The obvious singles at 630.1 and 620.3 eV are belong to the I3d and I5d of iodine molecular, while the peaks at 631.8 and 618.6 eV originated from the covalent bound iodine.[43]

The iodine capture capabilities of POPs in *n*-hexane solution were further monitored by UV-vis spectra (Fig. S9, ESI†). When samples (16 mg) were immersed in this iodine solution (2 mL, 8.0 mM), the purple solution was observed to fade gradually to paler with the extension of adsorption time, accompanied with the colour of sorbents deepening gradually (Fig. S10, ESI†). The colour of the solution became colourless when interacting with **TatPOP-2** after 6 h, indicating that the iodine in solution can be rapidly and efficiently captured. Nevertheless, no drastically colour change was viewed for **MelPOP-2** after 6 h. The result implies that the ability of iodine adsorption for **TatPOP-2** was stronger than that of **MelPOP-2**. This result implicates that **TatPOP-2** with longer conjugated unit has stronger interaction towards iodine than that of **MelPOP-2**, which accelerated the iodine loading speed. To provide further information about the interactions between host and guest molecular, adsorption isotherms (Fig.3b) were implemented at room temperature. As expected from the kinetic studies, TatPOP-2 and MelPOP-2 present the unprecedentedly high sorption capacity with iodine uptake of 1239 mg/g and 764 mg/g, respectively. To our best of knowledge, this iodine adsorption ability surpasses almost all of the known porous materials.

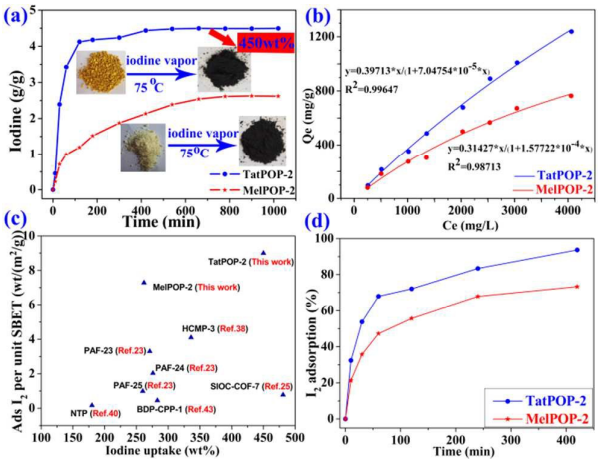

Fig.3 a) Iodine vapor adsorption curves of POPs at various time intervals; b) Iodine adsorption isotherms at room temperature (Langmuir model); Ce: iodine concentration at equilibrium; Qe: iodine adsorbed quantity; c) Iodine uptakes (1 bar) and per unit SBET for iodine adsorption; d) Iodine adsorption curves of POPs (16 mg) at various time intervals in iodine-hexane solution (8 mM, 2 mL, 25 °C).

As shown in Fig 3d, the captures of iodine in *n*-hexane solution for **MelTOP-2** and **TatPOP-2** were close to 74% and 94% with a sufficient contact time (7 h), respectively. The iodine molecule loaded in the porous matrix can be readily-easily released in organic solvents (Fig. S11, ESI†) like ethanol and the desorption equilibrium was attained in one hour in ethanol. The iodine released rate of POPs adsorbents increased linearly in the primitively 30 min, showing the release of **MelPOP-2** is quicker than that of **TatPOP-2**, as reflected by their linear slopes (Fig. S13, ESI†). Similar trend on the host-guest interaction also can be exhibited by the desorption experiments. Additionally, the POPs samples can be easily

View Article Online
DOI: 10.1039/C8CC04242J

regenerated & reused for next round of adsorption behind washing and controlled releasing for the practical applications.

In summary, two conjugated nanoporous polymers with good stability were constructed using a catalysis-free one-spot polymerization of HCCP with melamine/TAPT. Their iodine adsorption capacity could be effectively improved via methodically extending π-conjugated chain. This can be considered as a direct and effective strategy to achieve high iodine loading amount in nanoporous polymers. Taking into account the advantages of the extended *p*–π conjugated structure and heteroatom-rich backbone, an ultrahigh iodine capture of up to 450 wt% was achieved for our frameworks. These results indicate that incorporating extended π-conjugated units into frameworks is favourable to enhance the iodine adsorption of the porous organic polymers. These attracting properties make them promising candidates for radioactive iodine capture and sequestration to address environmental issues.

We acknowledge the financially support from the National Science Foundation of China (Nos. 21674129, 21376272 and 21636010), the Hunan Provincial Science and Technology Plan Project, China (No.2016TP1007), Joint Funds of Hunan Provincial Natural Science Foundation and ZhuZhou Municipal Government of China (2015JJ5010).

Conflicts of interest

There are no conflicts to declare

Notes and references

1 N. Yoshida and J. Kanda, *Science.*, 2012, **336**, 1115–1116.
2 P. C. Burns, R. C. Ewing and A. Navrotsky, *Science.*, 2012, **335**, 1184–1188.
3 D. F. Sava, M. A. Rodriguez, K. W. Chapman, P. J. Chupas, J. A. Greathouse, P. S. Crozier and T. M. Nenoff, *J. Am. Chem. Soc.*, 2011, **133**, 12398–12401.
4 K. S. Subrahmanyam, D. Sarma, C. D. Malliakas, K. Polychronopoulou, B. J. Riley, D. A. Pierce, J. Chun and M. G. Kanatzidis, *Chem. Mater.*, 2015, **27**, 2619–2626.
5 J. Zhou, S. Hao, L. Gao and Y. Zhang, *Ann. Nucl. Energy*, 2014, **72**, 237–241.
6 N. V. Nguyen, J. Jeong, D. Shin, B.-S. Kim, J. Lee and B. D. Pandey, *Mater. Trans.*, 2012, **53**, 760–765.
7 T. Hertzsch, F. Budde, E. Weber and J. Hulliger, *Angew. Chemie - Int. Ed.*, 2002, **41**, 2281–2284.
8 D. Banerjee, X. Chen, S. S. Lobanov, A. M. Plonka, X. Chan, J. A. Daly, T. Kim, P. K. Thallapally and J. B. Parise, *ACS Appl. Mater. Interfaces*, 2018, **10**, 10622–10626.
9 X. Zhang, I. da Silva, H. G. W. Godfrey, S. K. Callear, S. A. Sapchenko, Y. Cheng, I. Vitórica-Yrezábal, M. D. Frogley, G. Cinque, C. C. Tang, C. Giacobbe, C. Dejoie, S. Rudić, A. J. Ramirez-Cuesta, M. A. Denecke, S. Yang and M. Schröder, *J. Am. Chem. Soc.*, 2017, **139**, 16289–16296.
10 H. Li, X. Ding and B.-H. Han, *Chem. - A Eur. J.*, 2016, **22**, 11863–11868.
11 Y. Liao, Z. Cheng, W. Zuo, A. Thomas and C. F. J. Faul, *ACS Appl. Mater. Interfaces*, 2017, **9**, 38390–38400.
12 Q.-Q. Dang, H.-J. Wan and X.-M. Zhang, *ACS Appl. Mater. Interfaces*, 2017, **9**, 21438–21446.
13 X. Guo, Y. Tian, M. Zhang, Y. Li, R. Wen, X. Li, X. Li, Y. Xue, L. Ma, C. Xia and S. Li, *Chem. Mater.*, 2018, ***30***, 2299–2308.
14 S. A, Y. Zhang, Z. Li, H. Xia, M. Xue, X. Liu and Y. Mu, *Chem. Commun.*, 2014, **50**, 8495–8498.
15 Y. Lin, X. Jiang, S. T. Kim, S. B. Alahakoon, X. Hou, Z. Zhang, C. M. Thompson, R. A. Smaldone and C. Ke, *J. Am. Chem. Soc.*, 2017, **139**, 7172–7175.
16 S. Das, P. Heasman, T. Ben and S. Qiu, *Chem. Rev.*, 2017, **117**, 1515–1563.
17 Y. Xu, S. Jin, H. Xu, A. Nagai and D. Jiang, *Chem. Soc. Rev.*, 2013, **42**, 8012-8031.
18. G. Li, Q. Liu, B. Xia, J. Huang, S. Li, Y. Guan, H. Zhou, B. Liao, Z. Zhou and B. Liu, *Eur. Polym. J.*, 2017, **91**, 242–247.
19 D. Chen, Y. Fu, W. Yu, G. Yu and C. Pan, *Chem. Eng. J.*, 2018, **334**, 900–906.
20 C. Pei, T. Ben, S. Xu and S. Qiu, *J. Mater. Chem. A*, 2014, **2**, 7179–7187.
21 M. G. Rabbani and H. M. El-Kaderi, *Chem. Mater.*, 2011, **23**, 1650–1653.
22 W. Lu, J. P. Sculley, D. Yuan, R. Krishna, Z. Wei and H.-C. Zhou, *Angew. Chemie - Int. Ed.*, 2012, **51**, 7480–7484.
23 Z. Yan, Y. Yuan, Y. Tian, D. Zhang and G. Zhu, *Angew. Chemie - Int. Ed.*, 2015, **54**, 12733–12737.
24 Y. Chen, H. Sun, R. Yang, T. Wang, C. Pei, Z. Xiang, Z. Zhu, W. Liang, A. Li and W. Deng, *J. Mater. Chem. A*, 2015, **3**, 87–91.
25 Z.-J. Yin, S.-Q. Xu, T.-G. Zhan, Q.-Y. Qi, Z.-Q. Wu and X. Zhao, *Chem. Commun.*, 2017, **53**, 7266–7269.
26 F. Ren, Z. Zhu, X. Qian, W. Liang, P. Mu, H. Sun, J. Liu and A. Li, *Chem. Commun.*, 2016, **52**, 9797–9800.
27 B. Li, Y. Zhang, R. Krishna, K. Yao, Y. Han, Z. Wu, D. Ma, Z. Shi, T. Pham, B. Space, J. Liu, P. K. Thallapally, J. Liu, M. Chrzanowski and S. Ma, *J. Am. Chem. Soc.*, 2014, **136**, 8654–8660.
28 X. Qian, B. Wang, Z. Zhu, H. Sun, F. Ren, P. Mu, C. Ma, W. Liang and A. Li, *J. Hazard. Mater.*, 2017, **338**, 224–232.
29 H. Sun, P. La, R. Yang, Z. Zhu, W. Liang, B. Yang, A. Li and W. Deng, *J. Hazard. Mater.*, 2017, **321**, 210–217.
30 Y. H. Abdelmoaty, T. Tessema, F. A. Choudhury, O. M. El-Kadri and H. M. El-Kaderi, *ACS Appl. Mater. Interfaces*, 2018, **10**, 16049–16058.
31 S. Zhang, X. Zhao, B. Li, C. Bai, Y. Li, L. Wang, R. Wen, M. Zhang, L. Ma and S. Li, *J. Hazard. Mater.*, 2016, **314**, 95–104.
32 Q.-Q. Dang, X.-M. Wang, Y.-F. Zhan and X.-M. Zhang, *Polym. Chem.*, 2016, **7**, 643–647.
33 S. U. Nandanwar, K. Coldsnow, V. Utgikar, P. Sabharwall and D. Eric Aston, *Chem. Eng. J.*, 2016, **306**, 369–381.
34 D.-H. Lan, H.-T. Wang, L. Chen, C.-T. Au and S.-F. Yin, *Carbon N. Y.*, 2016, **100**, 81–89.
35 S. Ren, Q. Fang, Y. Lei, H. Fu, X. Chen, J. Du and A. Cao, *Macromol. Rapid Commun.*, 2005, **26**, 998–1001.
36 T. Pan, X. Huang, H. Wei, W. Wei and X. Tang, *Macromol. Chem. Phys.*, 2012, **213**, 1590–1595.
37 M. Thommes, K. Kaneko, A. V. Neimark, J. P. Olivier, F. Rodriguez-Reinoso, J. Rouquerol and K. S. W. Sing, *Pure Appl. Chem.*, 2015, **87**, 1051–1069.
38 Y. Liao, J. Weber, B. M. Mills, Z. Ren and C. F. J. Faul, *Macromolecules*, 2016, **49**, 6322–6333.
39 T. Ben, H. Ren, S. Ma, D. Cao, J. Lan, X. Jing, W. Wang, J. Xu, F. Deng, J. M. Simmons, S. Qiu and G. Zhu, *Angew. Chemie*, 2009, **121**, 9621–9624.
40 H. Ma, J.-J. Chen, L. Tan, J.-H. Bu, Y. Zhu, B. Tan and C. Zhang, *ACS Macro Lett.*, 2016, **5**, 1039–1043.
41 M.-H. Zeng, Q.-X. Wang, Y.-X. Tan, S. Hu, H.-X. Zhao, L.-S. Long and M. Kurmoo, *J. Am. Chem. Soc.*, 2010, **132**, 2561–2563.
42 G. Deboer, J. W. Burnett and M. A. Young, *Chem. Phys. Lett.*, 1996, **259**, 368–374.
43 Y. Zhu, Y.-J. Ji, D.-G. Wang, Y. Zhang, H. Tang, X.-R. Jia, M. Song, G. Yu and G.-C. Kuang, *J. Mater. Chem. A*, 2017, **5**, 6622–6629.

